



ELSEVIER

Journal of Photochemistry and Photobiology A: Chemistry 122 (1999) 17–22

Journal of  
Photochemistry  
and  
Photobiology  
A: Chemistry

## A new diolefinic laser dye: 2,5-bis-2-(2-naphthyl) vinyl pyrazine (B2NVP)

Sadiq M. Al-Hazmy<sup>a,\*</sup>, A.S. Babaqi<sup>a</sup>, E. Daltrozzo<sup>b</sup>, M. Klink<sup>b</sup>, J. Sauter<sup>b</sup>, E.M. Ebeid<sup>c</sup>

<sup>a</sup>Department of Chemistry, Faculty of Science, Sana'a University, Sana'a, Yemen

<sup>b</sup>Fakultät für Chemie, Universität Konstanz, Konstanz, Germany

<sup>c</sup>Department of Chemistry, Faculty of Science, Tanta University, Tanta, Egypt

Received 28 October 1998; accepted 4 November 1998

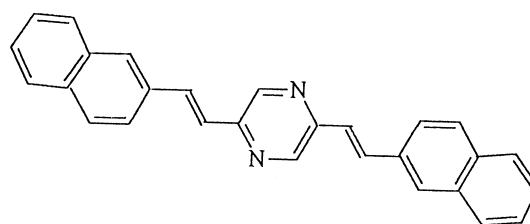
### Abstract

The title dye acts as a laser dye upon pumping with nitrogen laser ( $\lambda_{\text{ex}} = 337.1$ ). B2NVP in *N,N*-dimethylformamide (DMF) gives amplified spontaneous emission (ASE) with a maximum at about 470 nm, but only low laser activity upon nitrogen laser pumping. The difference between  $\sigma_{\text{E}}$  (emission cross-section) and  $\sigma_{\text{E}}^*$  (from ASE calculated effective emission cross-section) is interpreted as  $S_1$ – $S_n$  absorption, the maximum of this absorption occurring in DMF at around 500 nm. Thereby the laser efficiency of the dye is strongly reduced. Investigations on the photochemical stability, photochemical quantum yields, and the dependence efficiency of the dye. B2NVP has short excited state lifetimes, high fluorescence efficiencies and low photochemical quantum yields. The dye undergoes solubilization in anionic micelles with subsequent increase in fluorescence efficiencies. Energy transfer from B2NVP to rhodamine6G (R6G) in dimethylsulfoxide (DMSO) has been studied giving a second order quenching rate constant of  $8.7 \times 10^{13} \text{ M}^{-1} \text{ s}^{-1}$ . © 1999 Elsevier Science S.A. All rights reserved.

**Keywords:** Diolefins; Amplified spontaneous emission

### 1. Introduction

Diolefinic compounds containing pyrazinyl moieties have been reported as important candidates in many research areas. 2,5-distyrylpyrazine (DSP) was the first reported derivative to undergo solid-state four-center photopolymerization giving highly crystalline polymer [1–3]. Members of this family of compounds have been recently reported as organic electroluminescent crystals giving high brightness at low DC voltage of about 10 V [4]. One of the most important applications of these compounds is their use as laser dyes. Laser emission from DSP [5] and 1,4-bis( $\beta$ -pyrazinyl-2-vinyl) benzene (BPVB) was observed [6] upon pumping concentrated solutions of these dyes using a nitrogen laser source. The naphthyl analog of DSP is expected to emit at longer wavelengths and to show a strongly supposed *trans*–*cis* isomerization process [7] due to changes in bond lengths on going from the  $S_0$  to the  $S_1$  state. In this communication we report the emission characteristics, lifetime and amplified spontaneous emission of 2,5-bis-2-(2-naphthyl) vinylpyrazine (B2NVP).



B2NVP

### 2. Experimental

The final crystallization of B2NVP<sup>1</sup> was from xylene (mp 319–320°C). Fluorescence spectra and fluorescence quantum yields ( $\phi_f$ ) were measured using a Shimadzu RF 510 spectrofluorophotometer using diphenylanthracene and quinine sulphate as reference standards [8]. Quantum yields of the *trans*–*cis* photoisomerization of B2NVP ( $\phi_c$ ) were measured using a modified method that takes into account the

\*Corresponding author.

<sup>1</sup>The B2NVP sample was kindly provided by Professor Masaki Hasegawa of Toin University, Yokohama, Japan.

change in absorbance with proceeding photoisomerization [9].

UV–Vis absorption spectra were measured using a Shimadzu UV-1200 S spectrophotometer. Fluorescence lifetimes were measured by the single photon counting technique using an air flash lamp operating between 20 and 40 kHz. Excitation wavelengths were selected using a bandpass filter (260–380 nm), the emission wavelengths were selected by appropriate filters (Schott, Mainz, Germany). The data were registered in a 1000 channels analyzer with a resolution of 24 channels/ns. The decay profiles were analyzed by iterative convolution using autocorrelation and residual criteria [10]. ASE was measured using a nitrogen laser (type 1M 50A, Lambda Physics;  $\lambda_{\text{ex}} = 337.1$  nm, pulse duration = 5 ns) as excitation source and an optical multi-channel analyzer (type OMA II, Princeton Applied Research Corp.) as detector [11]. The dye cuvette was placed in the focus of a cylindrical lens, which concentrates the  $N_2$  laser beam to a narrow line. The dye concentration was  $6.32 \times 10^{-5}$  M in DMF solvent. Eight ASE spectra were recorded for different pulse energies (between 0.1 and 1.5 mJ). All spectra were measured in the unsaturated light amplification region. Within the model used [11], the relation between ASE intensity  $I$  and excitation pulse intensity  $P$  is given by equations (Eqs. (1)–(3)):

$$I(L, \lambda, P) = F(\lambda)N_1(P) \int_0^L \exp[N_1(P)\sigma_E^*(\lambda) - N_0(P)\sigma_A(\lambda)] dx \quad (1)$$

$$N_1(P) = N \frac{\sigma_{\text{ex}}k_{\tau}P}{\sigma_{\text{ex}}k_{\tau}P + 1/\tau} \quad (2)$$

$$N = N_0 + N_1 \quad (3)$$

where  $N$  is the total dye concentration in molecules/cm<sup>3</sup>,  $N_0$  and  $N_1$  are the populations of the ground state ( $S_0$ ) and the

first excited singlet state ( $S_1$ ) respectively,  $\sigma_A$  is the absorption cross-section of the  $S_0$ ,  $\sigma_{\text{ex}}$  is  $\sigma_A$  at 337.1 nm,  $\sigma_E^*$  is the effective emission cross-section,  $L$  is the length of the excited region within the dye cuvette (16–19 mm),  $\tau$  is the lifetime of the  $S_1$  state,  $k_{\tau}$  is a correction factor and  $F$  is a factor depending on fluorescence intensity, detector sensitivity, and geometrical conditions. The factor  $k_{\tau}$  gives the deviation of  $N_1$  from the value obtainable under steady state conditions and depends on the ratio excitation pulse duration to  $S_1$  lifetime  $\tau$ . The difference between  $\sigma_E^*$  (effective emission cross-section) and  $\sigma_E$  (emission cross-section) we interpret as the absorption cross sections  $\sigma_A^*$  of  $S_n \leftarrow S_1$  transitions.  $F$  as well as  $\sigma_E^*$  are determined from the ASE spectra by curve fitting. The emission cross section  $\sigma_E$  is calculated from relation (Eq. (4)), where  $E$  means the normalized fluorescence lineshape function, which is correlated with fluorescence quantum yield  $\phi_f$  by equation (Eq. (5)).

$$\sigma_E(\lambda) = \frac{E(\lambda)\lambda^4}{8\pi\tau cn^2} \quad (4)$$

$$\int E(\lambda) d\lambda = \phi_f \quad (5)$$

where  $n$  is the refractive index of the dye solution,  $c$  is the velocity of light in vacuum,  $E(\lambda)$  is obtained from solutions whose absorptivities are low to avoid reabsorption processes (optical density at absorption maximum  $\leq 0.1$ ). The excited state absorption cross-section  $\sigma_A^*$  is calculated from the difference ( $\sigma_E - \sigma_E^*$ ) [11].

### 3. Results and discussion

Table 1 summarizes some spectral data of B2NVP in different solvents. The absorption of B2NVP is not strongly affected by solvent polarity, whereas the emission spectra

Table 1  
Spectral data,  $\phi_f$  and  $\phi_c$  values of B2NVP in different solvents

| Solvent                         | $\lambda_{\text{max}}$ (F). (nm) | $\lambda_{\text{max}}$ (abs) (nm) | $\epsilon$ (M <sup>-1</sup> cm <sup>-1</sup> ) |                 |                 | $\phi_f$                 |                 | $\phi_c$             | pK   | pK <sup>*</sup> |
|---------------------------------|----------------------------------|-----------------------------------|--|-----------------|-----------------|--------------------------|-----------------|----------------------|------|-----------------|
|                                 |                                  |                                   | $\lambda_{(\text{max})}$                       | $\lambda_{336}$ | $\lambda_{337}$ | $\lambda_{(\text{max})}$ | $\lambda_{337}$ |                      |      |                 |
| DMF                             | 462                              | 402                               | 45 700   | 27 200          | 14 500          | 0.51                     | 0.47            | $1.9 \times 10^{-3}$ | 2.16 | 1.79            |
| Ethylene glycol                 | 484                              | 406                               | –  | –               | –               | 0.56                     | 0.60            | –                    | –    | –               |
| CH <sub>3</sub> CN              | 457                              | 393                               | –  | –               | –               | 0.49                     | 0.42            | –                    | –    | –               |
| Isopropanol                     | 476                              | 399                               | 42 700   | 26 300          | 15 400          | 0.54                     | 0.41            | $7.0 \times 10^{-4}$ | –    | –               |
| CH <sub>2</sub> Cl <sub>2</sub> | 458                              | 397.5                             | –  | –               | –               | 0.61                     | 0.40            | –                    | –    | –               |
| Dioxane                         | 450                              | 398.5                             | –  | –               | –               | 0.51                     | 0.40            | –                    | –    | –               |
| CHCl <sub>3</sub>               | 464                              | 402                               | –  | –               | –               | 0.57                     | 0.26            | –                    | –    | –               |
| CCl <sub>4</sub>                | 451                              | 402.5                             | –  | –               | –               | 0.21                     | 0.13            | –                    | –    | –               |
| O/W                             | 468                              | 401.5                             | 32 100   | –               | –               | –                        | –               | $1.4 \times 10^{-3}$ | –    | –               |
| EtOH                            | 472                              | –                                 | –  | –               | –               | 0.64                     | 0.45            | –                    | –    | –               |
| MeOH                            | 482                              | 397                               | 41 000   | –               | –               | 0.65                     | 0.42            | –                    | –    | –               |
| Acetone                         | –                                | –                                 | –  | –               | –               | 0.64                     | 0.58            | –                    | –    | –               |
| BuOH                            | –                                | –                                 | –  | –               | –               | 0.75                     | 0.46            | –                    | –    | –               |
| <i>n</i> -Hexane                | 448                              | 401                               | –  | –               | –               | –                        | –               | –                    | –    | –               |
| DMSO                            | 470                              | 398.5                             | –  | –               | –               | 0.74                     | 0.57            | –                    | –    | –               |

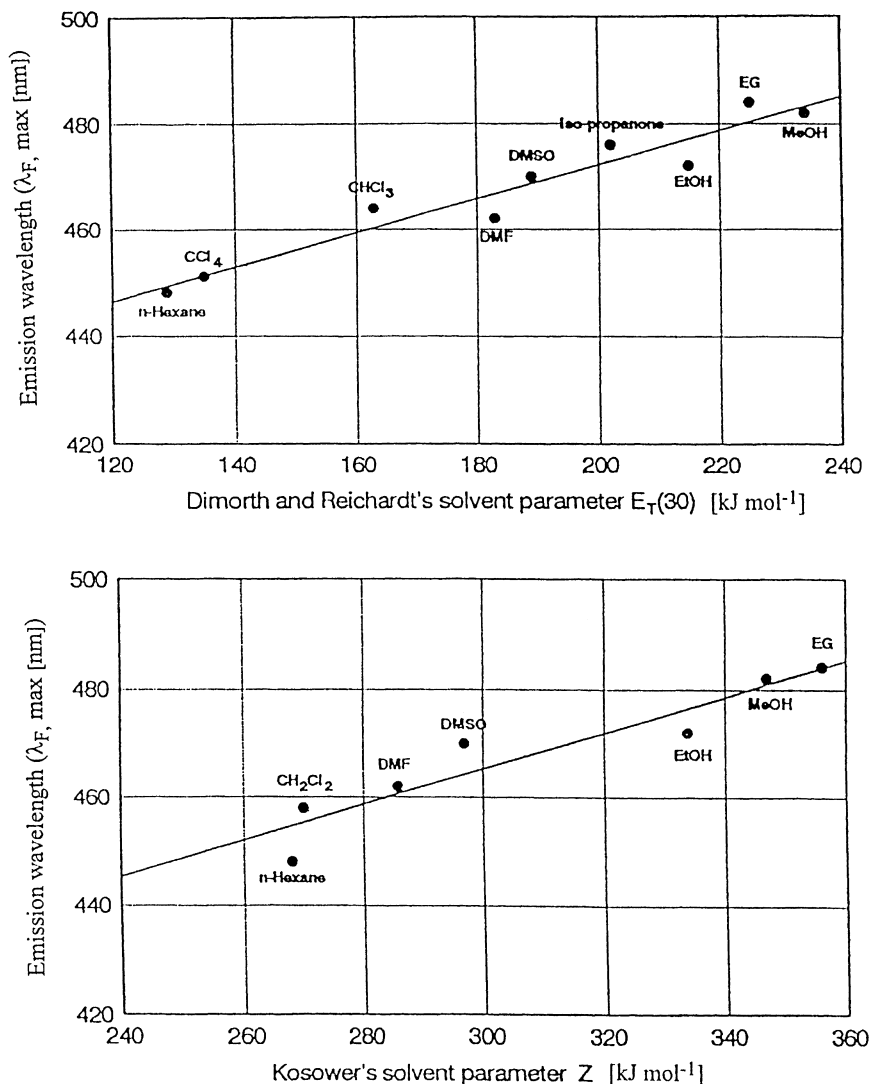


Fig. 1. Plot of emission maxima of B2NVP against (a) Dimroth–Reichardt's solvent parameter  $E_T$  and (b) Kosower's solvent parameter  $Z$ .

are significantly influenced by the medium. With increasing solvent polarity, the fluorescence maximum shifts to longer wavelengths from 448 nm in *n*-hexane ( $E_T = 129 \text{ kJ mol}^{-1}$ ) to 484 nm in ethylene glycol ( $E_T = 225 \text{ kJ mol}^{-1}$ ). In Fig. 1 the fluorescence maxima are plotted against Dimroth–Reichardt's ( $E_T$ ) and also against Kosower's solvent parameters ( $Z$ ) [12,13]. Due to hindrance around the naphthyl ethylenic bonds, the existence of different rotamers has to be taken in account. The existence of such rotamers is substantiated by both semiempirical calculations and the non-structured broad  $S_0$ – $S_1$  absorption as well as the dependence of the fluorescence and fluorescence excitation spectra on the exciting and observing wavelengths. Likewise, the fluorescence quantum yields are wavelength-dependent. This phenomena could be ascribed to two different, energetically preferred rotamers (conformers).

B2NVP undergoes solubilization in anionic micelles (sodium dodecyl sulphate (SDS)) The solubilization process is associated with an increase in the fluorescence intensity as

shown in Fig. 2. Plots of the surfactant concentrations versus fluorescence intensities of the dye show a distinct increase in fluorescence intensities at surfactant concentration corresponding to the critical micelle concentration (cmc) of SDS. This is shown in Fig. 2.

The protonation constant of the ground state ( $\text{p}K$ ) was calculated using relation (Eq. (6))

$$\text{pH} = \text{p}K - \log \frac{[\text{B}]}{[\text{BH}^+]} \quad (6)$$

where  $[\text{B}]$  is the concentration of the non-protonated form expressed in terms of its absorbance at 395 nm,  $[\text{BH}^+]$  is the concentration of the protonated form expressed in terms of the decrease in absorbance at 395 nm.

The protonation constants of the excited state  $\text{p}K^*$  were calculated using relation Eq. (7) [14]:

$$\text{p}K - \text{p}K^* = 2.10 \times 10^{-3} (\bar{\nu}_{\text{BH}^+} - \bar{\nu}_{\text{B}}) \quad (7)$$

The quantities  $\bar{\nu}_{\text{BH}^+}$ ,  $\bar{\nu}_{\text{B}}$  represent the wave numbers of (pure)

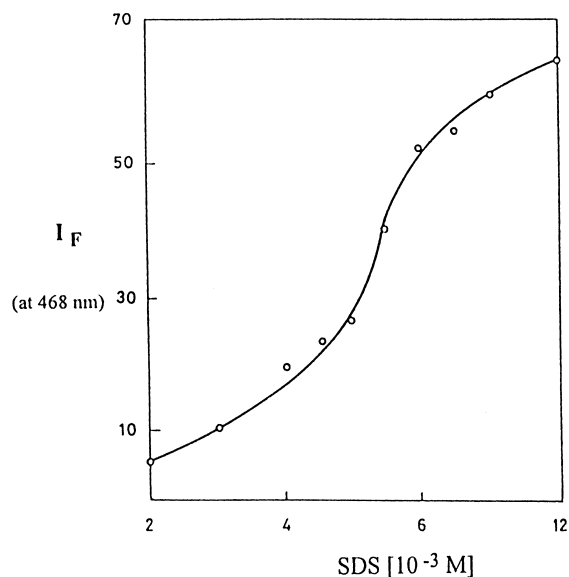


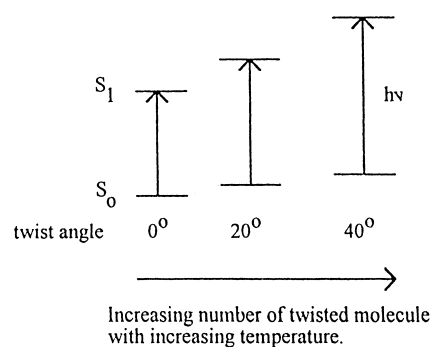
Fig. 2. Effect of concentration of SDS on the fluorescence intensity  $I_f$  of  $10^{-5}$  M solutions of B2NVP.

electronic transitions in acid and conjugate base, respectively. The wave numbers obtained from electronic absorption spectra give  $pK^*$  values, termed  $pK_{ab}^*$ . Wave numbers obtained from fluorescence spectra give  $pK^*$  values, termed  $pK_f^*$ . For B2NVP in DMF  $pK = 2.16$  and  $pK_{ab}^* = 1.79$  are determined.

From quantum chemical calculation, the bond order between the naphthalene and the ethylenic moiety increases in the excited state leading to reduction of rotational fre-

quencies with the consequence of rather high fluorescence quantum yield.

The absorption spectra of B2NVP in ethanol show a red shift of  $\approx 23$  nm is going from room temperature to 125 K. This is explainable by low rotational barriers for the naphthalene–ethylenic bonds in the ground state resulting in an equilibrium between the coplanar and twisted conformations. Due to strengthening of these very bonds in the  $S_1$  state, twisted conformers are at significantly higher energies compared with the energy of the coplanar. With lower temperatures the amount of coplanar molecules with correspondingly long wavelength absorption increases resulting in a long wavelength shift of the absorption band with decreasing temperature. Correspondingly, the half-width of the first electronic transition is reduced.



Saturated solutions of B2NVP in DMF give ASE with a maximum at 465 nm. The ground state absorption cross-section ( $\sigma_A$ ), the emission cross-section ( $\sigma_E$ ) as well as the effective emission cross section ( $\sigma_E^*$ ) are shown in Fig. 3.

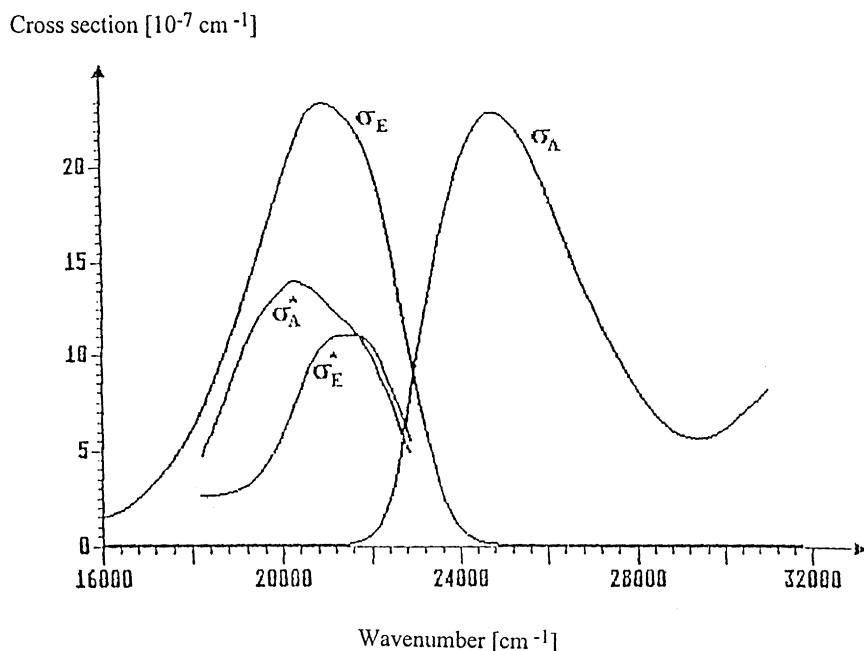


Fig. 3. The cross-sections (in units of  $cm^2$ ) for some processes of B2NVP in DMF.  $\sigma_A$  and  $\sigma_E$  are the ground state absorption and emission cross-sections, respectively.  $\sigma_A^*$  and  $\sigma_E^*$  are the excited state absorption cross section and the effective emission cross-section, respectively.

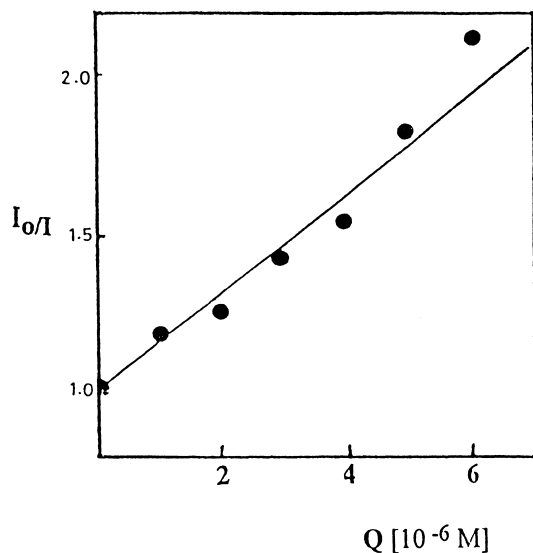


Fig. 4. Stern–Volmer plots for the quenching of B2NVP fluorescence using R6G as a quencher in DMSO at room temperature ( $\lambda_{\text{ex}} = 337$  nm,  $\lambda_{\text{em}} = 480$  nm). The concentration of B2NVP is  $5 \times 10^{-6}$  M.

The cross-section values are given in units of  $\text{cm}^2$ . The cross-section  $\sigma_A^*$  is given from the difference  $(\sigma_E - \sigma_E^*)$ . We interpret this difference as the first excited singlet state absorption band which reduces dye laser efficiency. Members of the diolefinic laser dye series containing pyridyl moieties e.g. 1,4-bis( $\beta$ -pyridyl-2-vinyl)benzene (P2VB) and its iso-electronic dye 1,4-bis(4-pyridyl-2-vinyl) benzene (P4VB) are more efficient laser dyes compared with B2NVP, BPVB and DSP because of significantly higher  $\sigma_E^*$  values and low  $\sigma_A^*$  values [11].

The B2NVP/rhodamine6G (B2NVP/R6G) system represents a useful energy transfer dye laser (ETDL) system achieving better harvesting of light photons at 337.1 nm (the wavelength of pumping nitrogen laser). Fig. 4 shows the Stern–Volmer plot of B2NVP fluorescence quenching using R6G as a quencher. The Stern–Volmer relation (Eq. (8))

$$\frac{I_0}{I} = 1 + k_q \tau_f [Q] \quad (8)$$

where  $I_0$  and  $I$  are the fluorescence intensities in the absence and presence of quencher of concentration  $[Q]$  ( $\text{mol dm}^{-3}$ ),  $k_q$  ( $\text{dm}^3 \text{mol}^{-1} \text{s}^{-1}$ ) the second-order quenching rate constant and  $\tau_f$  the fluorescence lifetime which is taken as 1.32 ns in DMSO [15]. From the slope (Fig. 4)  $k_q$  is calculated to be  $12 \times 10^{13} \text{ dm}^3 \text{mol}^{-1} \text{s}^{-1}$ . This value is much higher than the diffusion rate constant ( $k_{\text{diff}}$ ) in DMSO ( $0.37 \times 10^{10} \text{ dm}^3 \text{mol}^{-1} \text{s}^{-1}$ ) at room temperature. The high quenching rate constant value together with the overlap of the donor emission and the acceptor absorption indicate a diffusionless energy transfer mechanism. The emission intensity of donor in the presence of acceptor (R6G) was corrected against both reabsorption of donor emitted photons by R6G and absorption of excitation light by R6G using equations described earlier [16].

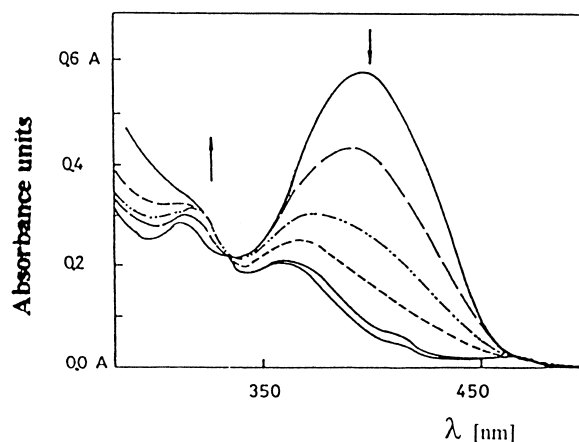


Fig. 5. Deterioration of B2NVP in  $\text{CCl}_4$  using 254 nm light in excitation. The changes in absorption spectra of  $1 \times 10^{-5}$  M solution of B2NVP in  $\text{CCl}_4$  as a result of UV irradiation ( $\lambda_{\text{ex}} = 254$  nm). The irradiation times at decreasing absorbance are 0, 2, 4, 6, 16 and 26 min.

The photostability of B2NVP has been studied in different media. The electronic absorption and emission spectra of B2NVP dilute solutions (ca.  $10^{-5} \text{ mol dm}^{-3}$ ) undergo change upon UV irradiation ( $\lambda_{\text{ex}} 365$  nm). The underlying photoreaction in such dilute solutions of diolefinic derivatives is interpreted as *trans-cis* photoisomerization. The photochemical quantum yield ( $\phi_c$ ) value in ethanol is given in Table 1. A rapid deterioration of the dye has been observed in carbon tetrachloride ( $\text{CCl}_4$ ) upon irradiation with 254 nm light as shown in Fig. 5. We propose an initial electron transfer from singlet excited B2NVP to  $\text{CCl}_4$  leading to the formation of a transient (exciplex). This is followed by the formation of an intermolecular ion pair  $[\text{B2NP}^+ \cdots \text{CCl}_4]$ , which gives  $[\text{B2NP}^+ \cdots \text{Cl} \cdots \text{CCl}_3]$  via the well-known  $\text{CCl}_4 + e \rightarrow \text{CCl}_3 + \text{Cl}^-$  reaction. The photostability of several electron donor molecules in halomethane solvents has been examined earlier [17–21].

## Acknowledgements

We thank Professor Masaki Hasegawa of Toin University of Yokohama, Japan for providing B2NVP sample.

## References

- [1] M. Hasegawa, Adv. Polym. Sci. 1 (1982).
- [2] M. Hasegawa, Chem. Rev. 83 (1983) 507.
- [3] H. Hasegawa, T. Katsumata, Y. Ito, K. Saigo, Y. Iitaka, Macromolecules 21 (1990) 3134.
- [4] M. Nohara, M. Hasegawa, C. Hosokawa, H. Tokallin, T. Kusumoto, Chem. Lett. 2 (1990) 189.
- [5] E.M. Ebeid, M.M.F. Sabry, S.A. El-Daly, Laser Chem. 5 (1985) 223.
- [6] E.M. Ebeid, R.M. Issa, S.A. El-Daly, M.M.F. Sabry, J. Chem. Soc., Faraday Trans. II 82 (1986) 1981.
- [7] M. Hasegawa, H. Harashina, T. Hosokawa, Jpn. Kokai Tokkyo Koho, Patent 89-75618, 27 March 1989.

- [8] J.V. Morris, M.A. Mahaney, J.R. Haber, *J. Phys. Chem.* 80 (1967) 969.
- [9] E.M. Ebeid, R.M. Issa, M.M. Ghoneim, S.A. El-Daly, *J. Chem. Soc., Faraday Trans. I* 82 (1986) 909.
- [10] J.N. Demas, *Excited State Lifetime Measurements*, Academic Press, New York, 1983, Chap. 6 and references therein.
- [11] M. Klink, Ph.D. Thesis, Universitat Konstanz, 1995.
- [12] C. Reichardt, E. Harbusch, *Liegigs Ann. Chem.* 721 (1983).
- [13] C. Reichardt, *Solvent and Solvent Effects in Organic Chemistry*, 2nd ed., VCH, Weinheim, Germany, 1988.
- [14] S.G. Schulman, *Modern Fluorescence Spectroscopy* E.L. Wehry, (Ed.), Plenum, New York, vol. 2, 1976.
- [15] V. Masilamani, B.M. Sivarani, *J. Lumin.* 27 (1982) 137.
- [16] B. Marciniak, *J. Chem. Edu.* 63(11) (1986) 998.
- [17] L. Wolinski, Z. Turzynski, K. Witkowski, *Makromol. Chem.* 188 (1987) 2895.
- [18] M.C. Biondic, R. Erra-Balsells, *J. Photochem. Photobiol. A: Chem.* 77 (1994) 149.
- [19] M.C. Biondic, R. Erra-Balsells, *J. Photochem. Photobiol. A: Chem.* 51 (1990) 341.
- [20] S. Matsuda, H. Kokado, E. Inoue, *Bull. Chem. Soc. Japan* 43 (1970) 2994.
- [21] R.E. Balsells, A.R. Farsca, *Aust. J. Chem.* 41 (1988) 104.